CLM-P845

CLM-P845

An Intelligent Shell for the Toroidal Pinch

C. M. Bishop

UK ATOMIC ENERGY AUTHORITY

Culham Laboratory

An Intelligent Shell for the Toroidal Pinch

C. M. Bishop.

Culham Laboratory, Abingdon, Oxfordshire OX14 3DB, UK
(EURATOM/UKAEA Fusion Association)

Abstract

Reversed field pinches are conventionally stabilised by surrounding the plasma with a thick metallic shell. This suppresses flux penetration but only for times shorter than the shell's resistive diffusion time. To improve on this we propose replacing the thick shell with an intelligent shell which provides active flux freezing on much longer time scales.

(Submitted for publication in Plasma Physics and Controlled Fusion)
June 1988

1 Introduction

Large scale stability in a reversed field pinch is generally achieved by surrounding the plasma with a close-fitting highly conducting shell. Macroscopic instabilities must drive flux through the shell and this sets up eddy currents which generate an opposing field distribution. On short time scales the flux through the shell remains fixed and growth of the unstable mode is inhibited. However, on longer time scales ohmic dissipation damps the eddy currents and allows flux to diffuse through the shell. Theoretical models (HENDER et al., 1986; GIMBLETT, 1986 and references therein) have shown that instabilities are only suppressed on time scales which are short compared to the long time constant of the shell (i.e., the characteristic time constant for penetration of vertical field). Recent experiments on HBTX1C (ALPER et al., 1988a) and OHTE (TAYLER et al., 1988) using thin shells with short time constants have confirmed these results and suggest that the plasma cannot be sustained for times much longer than some multiple of the shell time. Lowering the resistance of the shell increases the shell time constant so that, with a thick shell, resistive diffusion times of a few hundred milliseconds may be achieved. If the system is to be used as a reactor, however, much longer time scales, of the order of many seconds, will be required. To achieve this we propose a novel method of active flux freezing which creates, within certain limits, the effects of a perfectly conducting shell.

2 The Single Loop

We begin by considering how to freeze the total normal flux through a single conducting loop C. The flux is given by

$$\psi = \int_S \mathbf{B} \cdot d\mathbf{S} \tag{1}$$

where $\mathbf{B}$ is the total field, and $\mathbf{S}$ is any surface spanned by C. This flux may be split into two parts

$$\psi = \phi_e + \phi_r \tag{2}$$

where ϕ_e is the flux due to external currents, while ϕ_r arises from the current I flowing in the loop. From Ampere's law, ϕ_r is proportional to I and hence we may write

$$\phi_r = LI \tag{3}$$

whe L is the self inductance of the loop. Using Faraday's law we have

$$\frac{d\psi}{dt} = \int_S \frac{\partial \mathbf{B}}{\partial t} = -\oint \mathbf{E}.d\mathbf{l} = -\mathcal{E} \tag{4}$$

where $\mathcal{E}$ is the emf around the loop. Suppose we introduce a second 'sensing' loop geometrically concident with the first loop as shown in Fig.1. The sensing loop detects a voltage V_S given by the rate of change of total flux, so that $V_S = -\mathcal{E}$. This is fed to a linear amplifier whose output drives the main 'power' loop C. The circuit equation for the power loop is

$$\frac{d\psi}{dt} = -\mathcal{E} = V_R - IR \tag{5}$$

where R is the resistance of the loop. We take V_R to be a linear function of V_S

$$V_R = -(\alpha - 1)V_S. \tag{6}$$

where α is a constant describing the gain of the amplifier. Using eqs.(2) and (3) we have

$$\frac{d\phi_r}{dt} + (\frac{\Omega}{\alpha})\phi_r = -\frac{d\phi_e}{dt} \tag{7}$$

where $\Omega = R/L$ is the characteristic frequency of the power loop. Eq.(7) is easily solved for a general external flux source $\phi_e(t)$ to give

$$\begin{aligned} \phi_r(t) &= \phi_r(0)\exp\left\{-\left(\frac{\Omega}{\alpha}\right)t\right\} \\ &- \exp\left\{-\left(\frac{\Omega}{\alpha}\right)t\right\}\int_0^t dt' \exp\left\{\left(\frac{\Omega}{\alpha}\right)t'\right\}\frac{d}{dt'}\phi_e(t'). \end{aligned} \tag{8}$$

Consider a particular Fourier component of frequency ω:

$$\phi_e(t) = \phi_0\cos(\omega t) = \Re\left\{\phi_0 e^{i\omega t}\right\} \tag{9}$$

Then after the decay of any transients (the first term in eq.(8)) the response flux is given by

$$\begin{aligned} \phi_r(t) &= -\Re\left\{\frac{i\omega\phi_0 e^{i\omega t}}{i\omega + \Omega/\alpha}\right\} \\ &= \frac{\phi_0\left(\lambda\sin\omega t - \cos\omega t\right)}{[1+\lambda^2]} \end{aligned} \tag{10}$$

where $\lambda = (\Omega/\alpha\omega)$. As the amplification parameter α is increased, so $\lambda \to 0$ and $\phi_r \to -\phi_e$. Thus the total flux $\psi = \phi_e + \phi_r$ goes to zero. A simple resistive loop corresponds to $\alpha = 1$ and provides some degree of flux freezing, which improves as the resistance of the loop (and hence Ω) is decreased. However, there are practical limits to how small the resistance can be made. By providing feedback with $\alpha \gg 1$ substantially better suppression of flux penetration is easily achieved. This will be effective for Fourier components whose frequencies exceed a minimum value given by

$$\omega_{\min} = \Omega/\alpha \tag{11}$$

and again as α is increased so $\omega_{\min}$ can be made as small as desired. It is easily shown that the flux through the sensing loop remains frozen, in the limit $\alpha \gg 1$, even when the power and sensing loops are separated. An extension of this concept, to freeze the flux through a 'virtual' loop displaced a short distance from the wall, is described in the appendix.

We illustrate these results by considering a specific external flux given by

$$\phi_e(t) = \frac{1}{2}\{\cos\omega t + \cos 3\omega t\} \tag{12}$$

which is plotted, for $\omega = 1$, in Fig.2. In Fig.3 we plot (for $\Omega = 1$) the total flux $\psi = \phi_e + \phi_r$, for a resistive loop with no driving voltage (i.e., $\alpha = 1$). The total flux ψ is somewhat less than ϕ_e. (The dashed curve shows a decaying transient arising from the initial condition $\psi(t = 0) = 1$). The total flux with $\alpha = 10$ is plotted in Fig.4 and shows the substantially smaller flux penetration.

3 Stability considerations

Since the single loop of the previous section corresponds to an amplification circuit with feedback it is important to consider whether such a circuit will always be stable. For an ideal amplifier described by eq.(6) the exact expression for the response flux is given by eq.(8) and the stability of the system is clear. The imperfections of a practical amplifier can, however, induce instability and a general method for analysing this is provided by the Nyquist criterion. This requires a plot of the open circuit transfer function in the complex plane as a function of the input frequency.

To define the transfer function consider the sensing and power loops of section 2 to be well separated so that their mutual inductance is zero and there is no feedback. For an input flux

$$\phi_{in}(t) = \int_{-\infty}^{\infty} d\omega e^{i\omega t}\tilde{\phi}_{in}(\omega) \tag{13}$$

the output flux in Fourier space is given, from eqs.(3), (5) and (6), by

$$\tilde{\phi}_{out}(\omega) = G(\omega)\tilde{\phi}_{in}(\omega) \tag{14}$$

where the transfer function $G(\omega)$ is given by

$$G(\omega) = -\frac{(\alpha - 1)\omega(\omega + i\Omega)}{\omega^2 + \Omega^2} \tag{15}$$

Now consider the situation where the sensing and power loops coincide. Then for an external flux $\phi_e(t)$ the power loop generates a flux $\phi_r(t)$ while the sensing loop sees a flux $\phi_e(t)+\phi_r(t)$. Using eq. (14) we have, again in Fourier space,

$$\tilde{\phi}_r(\omega) = \frac{G(\omega)}{1 - G(\omega)} \tilde{\phi}_e(\omega). \tag{16}$$

Suppose the function $G(\omega)$ is plotted in the complex plane for real values of $\omega \in [-\infty, \infty]$. The Nyquist criterion states that the circuit will be stable unless this plot encloses the point $(1,0)$, corresponding to the poles $\omega = \omega_j$ where $G(\omega_j) = 1$ in eq.(16). For the idealised amplifier described by eq.(15) the Nyquist plot is shown in Fig.5a and the circuit is clearly stable. As an example of an imperfect amplifier, suppose that a time delay τ is introduced so that $V_R(t) = -(\alpha - 1)V_S(t - \tau)$. Then

$$G(\omega) = -\frac{(\alpha - 1)\omega(\omega + i\Omega)e^{-i\omega\tau}}{\Omega^2 + \omega^2} \tag{17}$$

which at large ω becomes a circle of radius $(\alpha - 1)$ which, for $\alpha \gg 1$, encloses the point $G = 1$ many times corresponding to the unstable modes with $\omega \sim (2n + 1)\pi/\tau$ (solid curve in Fig.5b). Stability may be restored by reducing the gain at large frequencies such that $\alpha(\omega) \to 0$ as $\omega \to \infty$, as shown schematically by the dashed curve in Fig.5b. In practice high frequencies can be dealt with by a thin shell, and it is straightforward to ensure stability without significantly reducing the performance of the circuit.

4 The Intelligent Shell

Consider a toroidal pinch surrounded by a grid as shown in Fig.6. Each plaquette in the grid is constructed like the single loop described in section 2 and independently freezes the total flux through that plaquette. The overall effect is equivalent to a perfectly conducting mesh for frequencies greater than $\omega_{\min}$. Modes with wavelengths shorter than the grid spacing will be largely unaffected, and this will determine the choice of the plaquette dimensions, both in the poloidal and toroidal directions, in terms of the spectrum of observed mode numbers.

Using the notation of section 2 the flux through the i^{th}loop may be written

$$\psi_i = \phi_{ei} + \phi_{ri} + \sum_{j \neq i}^{N} C_{ij}\phi_{rj} \tag{18}$$

where N is the total number of plaquettes, and C_{ij} describes the amount of flux penetrating the i^{th} plaquette due to a current flowing in the j^{th} plaquette. Eq.(18) is conveniently cast in vector notation:

$$\boldsymbol{\psi} = \boldsymbol{\phi}_e + (\mathbf{1} + \mathbf{C}) \cdot \boldsymbol{\phi}_r \tag{19}$$

where $\mathbf{1}$ denotes the unit matrix. The response of the amplifiers is given by

$$\mathbf{V}_R = -(\alpha - 1)\mathbf{V}_S \tag{20}$$

and hence the circuit equation for the grid can be written

$$(1+\mathbf{C})\cdot\frac{d}{dt}\phi_r+\left(\frac{\Omega}{\alpha}\right)\phi_r=-\frac{d}{dt}\phi_e \tag{21}$$

The solution of this equation is given by

$$\begin{aligned}\phi_r(t) &= \exp\left\{-\frac{\Omega}{\alpha}(1+\mathbf{C})^{-1}t\right\}\cdot\phi_r(0)\\ &- \exp\left\{-\frac{\Omega}{\alpha}(1+\mathbf{C})^{-1}t\right\}\cdot\\ &\int_0^t dt'\exp\left\{\frac{\Omega}{\alpha}(1+\mathbf{C})^{-1}t'\right\}\cdot(1+\mathbf{C})^{-1}\cdot\frac{d}{dt'}\phi_e(t')\end{aligned} \tag{22}$$

where the exponential of a matrix is defined by

$$\exp(\mathbf{M})\equiv\sum_{n=1}^{\infty}\frac{(\mathbf{M})^n}{n!}. \tag{23}$$

Again consider a single Fourier component

$$\phi_e(t)=\Re\left\{\phi_0 e^{i\omega t}\right\} \tag{24}$$

Then neglecting transients we have

$$\phi_r(t)=\Re\left\{-i\omega\left[i\omega(1+\mathbf{C})+\left(\frac{\Omega}{\alpha}\right)\mathbf{1}\right]^{-1}\cdot\phi_0 e^{i\omega t}\right\} \tag{25}$$

For $\alpha\gg 1$, we again have $\phi_r\simeq-(1+\mathbf{C})^{-1}\cdot\phi_e$ and hence the total flux $\psi\simeq 0$.

If required a given external flux $\phi_0(t)$ can be allowed to pass freely through the mesh by adding a voltage $\mathbf{V}_0(t)=\alpha(d\phi_0/dt)$ to the RHS of eq.(20). This cancels the induced emf allowing the flux to penetrate freely and without drawing power from the amplifier. With the conventional thick shell an external control field which penetrates the shell cannot be changed on a timescale faster than the shell time constant. This constraint is removed with the intelligent shell.

5 Conclusions

Recent experimental results, as well as theoretical models, suggest that the pulse duration of a reversed field pinch is limited to some small multiple of the resistive diffusion time of the conducting shell. This is typically very much shorter than the long pulse times required for a reactor. To solve this problem we introduce an active feedback system which reproduces, to some extent, the effects of a perfectly conducting wall. A simple extension of this concept generates a virtual shell situated a short distance inside the wall.

The technology for such a system already exists and will be used for feedback control of tearing modes in tokamaks (MONTICELLO et al., 1979; LAZZARO and NAVE, 1987).

This will be done by detecting the presence of a single tearing mode with specific poloidal and toroidal mode numbers and applying a feedback field, with carefully controlled phase, to suppress the mode. In many respects the intelligent shell for the reversed field pinch is a simpler system yet effectively deals with a whole spectrum of toroidal and poloidal mode numbers simultaneously as well as a wide range of frequencies.

In addition to providing active flux freezing on very long time scales the intelligent shell, unlike the conventional conducting wall, has no continuous electrical path around the torus. There is therefore no need to introduce the usual shell gap with consequent field errors and loss of axisymmetry. Indeed, apart from ripple due to the finite mesh spacing, the mesh is axisymmetric.

Acknowledgements

I would like to thank Dr. S. C. Cowley and Dr. C. G. Gimblett for valuable discussions, and also Dr. M. K. Bevir for suggesting the possibility of a virtual shell.

Appendix

The Virtual Shell

In the fully relaxed state of a toroidal plasma (TAYLOR 1974) the quantity $\mu \equiv \mathbf{J} \cdot \mathbf{B}/B^2$ (where J is the current density and B is the magnetic field) is constant over the whole plasma volume. In practice this does not occur since μ, though constant over most of the plasma, falls to zero in the edge region. By making the conducting shell a closer fit to the plasma, however, the plasma can more closely approach the Taylor state and this is manifested as a reduction in the loop volts for a given toroidal current (ALPER et al., 1988b). This procedure is limited, however, because the plasma edge must be in contact with a cold wall. A simple extension of the intelligent shell concept overcomes this problem by introducing a 'virtual shell' displaced a short distance inside the wall.

Consider first a single plaquette as in section 2. Defining $x = (r_w - r)$, where r is the minor radius variable and r_w is the minor radius of the power loop, we consider two sensing loops located at $x = x_1$ and $x = x_2$ as shown in Fig.7. The aim is to freeze the flux through the imaginary loop at $x = x_v$ by using the pair of sensing loops to detect the gradient of the radial field. This requires that we represent the radial field due to the plasma currents as a linear function of x, and this places a limit on how far the virtual shell can be displaced inwards from the wall. Higher coefficients in the Taylor expansion of $B_r(x)$ could be detected using extra sense coils at the price of increased complexity. The flux through the virtual loop, due to external sources, is therefore

$$\phi(x_v) = \left(\frac{x_v - x_2}{x_1 - x_2}\right)\phi_1 - \left(\frac{x_v - x_1}{x_1 - x_2}\right)\phi_2 \tag{26}$$

where ϕ_1 and ϕ_2 are the fluxes through the sense loops. We write the flux χ through the virtual loop due to the current I in the power loop as

$$\chi(x_v) = f(x_v)LI \tag{27}$$

where the mutual inductance function $f(x)$ satisfies $f(0) = 1$. The output voltages of the sensing loops are given by

$$\begin{aligned} V_1 &= \frac{d}{dt}(m_1 LI + \phi_1) \\ V_2 &= \frac{d}{dt}(m_2 LI + \phi_2) \end{aligned} \tag{28}$$

where $m_1 = f(x_1)$ and $m_2 = f(x_2)$. The circuit equation for the power loop is

$$\frac{d}{dt}\left(LI + \phi(0)\right) = V_R - IR \tag{29}$$

where the amplifier output V_R is a linear function of V_1 and V_2:

$$V_R = -(\alpha - 1)\,[V_1 + \mu V_2] \tag{30}$$

and μ is to be determined. Solving the equations as before we find, in the limit of large α,

$$(m_1 + \mu m_2)\chi(x_v) + (\phi_1 + \mu\phi_2)f(x_v) = \text{const.} \tag{31}$$

We now require $\chi(x_v) = -\phi(x_v)$, for any $\phi(x_v)$. Using eq.(26) and equating coefficients of ϕ_1 and ϕ_2 we find

$$\mu = -\left(\frac{x_v - x_1}{x_v - x_2}\right) \tag{32}$$

(as expected, since this gives the correct mix of ϕ_1 and ϕ_2 in eq.(30) to generate $\phi(x_v)$), together with

$$f(x_v) = P(x_v) \tag{33}$$

where

$$P(x) \equiv \left(\frac{x - x_2}{x_1 - x_2}\right) m_1 - \left(\frac{x - x_1}{x_1 - x_2}\right) m_2 \tag{34}$$

A graphical solution of eq.(33) is shown schematically in Fig.8. The solution (A) is $x_v = x_1$ which, from eq.(32), gives $\mu = 0$. This corresponds to flux frozen through the loop at x_1, with the loop at x_2 playing no role. Similarly solution (B) is $x_v = x_2$ which gives $\mu = \infty$ and corresponds to freezing the flux through the loop at x_2. There is a third, non-trivial, solution for x_v at (C), which, with the appropriate value of μ from eq.(32), gives frozen flux through the virtual loop. A mesh of such loops will create a virtual shell located a short distance inside the wall. This will freeze normal flux in so far as external fields (including those from other loops as well as from the plasma) can be represented as linear functions of x.

References

ALPER B. et al. (1988a) . *Proc. 15th. Europ. Conf. on Contr. Fusion and Plasma Physics (Dubrovnic)*, to be published.

ALPER B. et al. (1988b). *Plasma Physics and Controlled Fusion* , **30**, to appear.

GIMBLETT C. G. (1986). *Nucl. Fusion*, **26**, 617.

HENDER T. C. et al. (1986). *Proc. 13th. Europ. Conf. on Contr. Fusion and Plasma Physics (Schliersee)* , Vol.1, 61.

LAZZARO E. and NAVE M. F. F. (1987). *JET Report* JET-P(87)54 , JET Joint Undertaking, Abingdon, Oxon., OX14 3EA, UK.

MONTICELLO D. A. et al. (1979). *Proc. Conf. on Plasma Physics and Contr. Fusion (Innsbruck)*, IAEA Vienna Vol.1, 605.

TAYLER P. et al. (1988). *Proc. 15th. Europ. Conf. on Contr. Fusion and Plasma Physics (Dubrovnic)*, to be published.

TAYLOR J. B. (1974). *Phys. Rev. Lett.*, **33**, 1139.

TAYLOR J. B. (1974). *Phys. Rev. Lett.*, **33**, 1139.

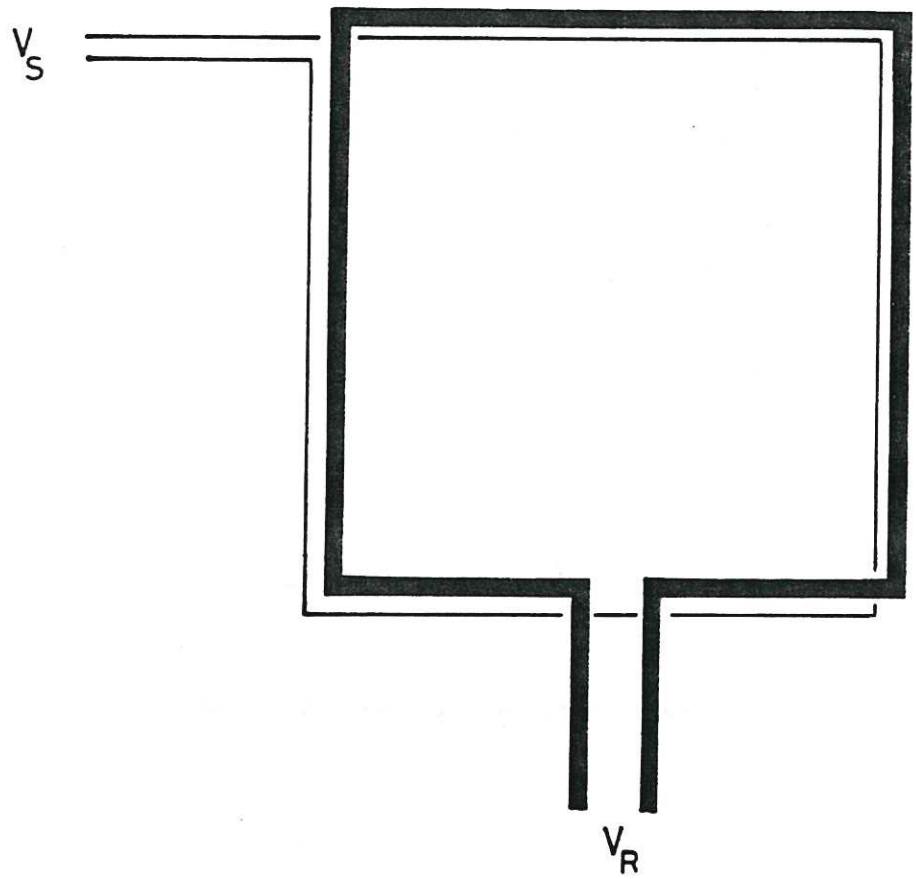

Fig. 1 Power loop together with associated sensing loop.

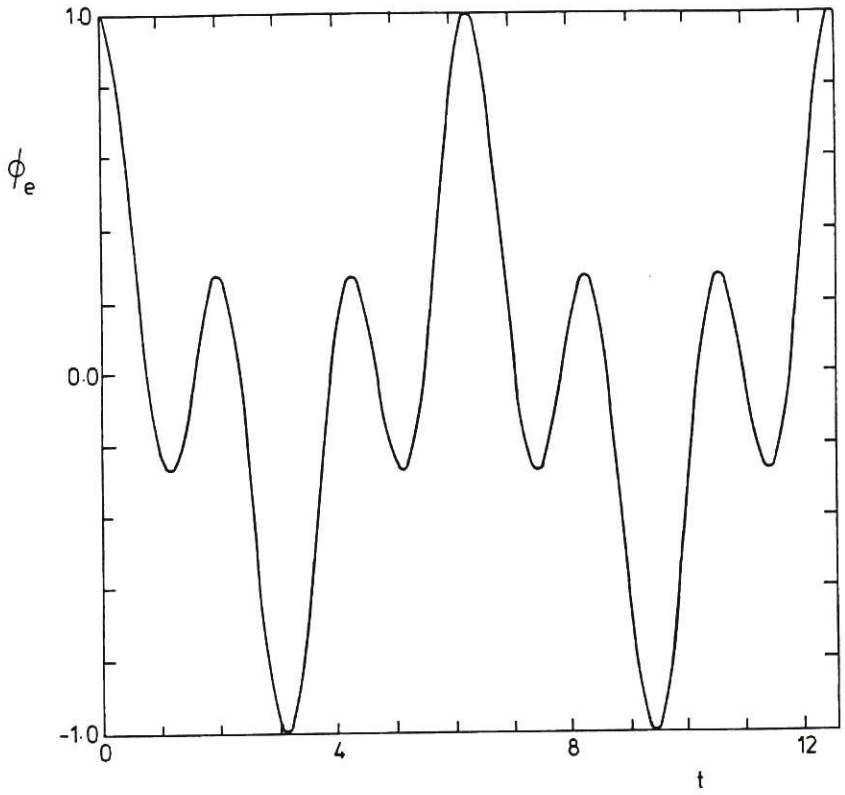

Fig. 2 Example of an external flux function ϕ_e.

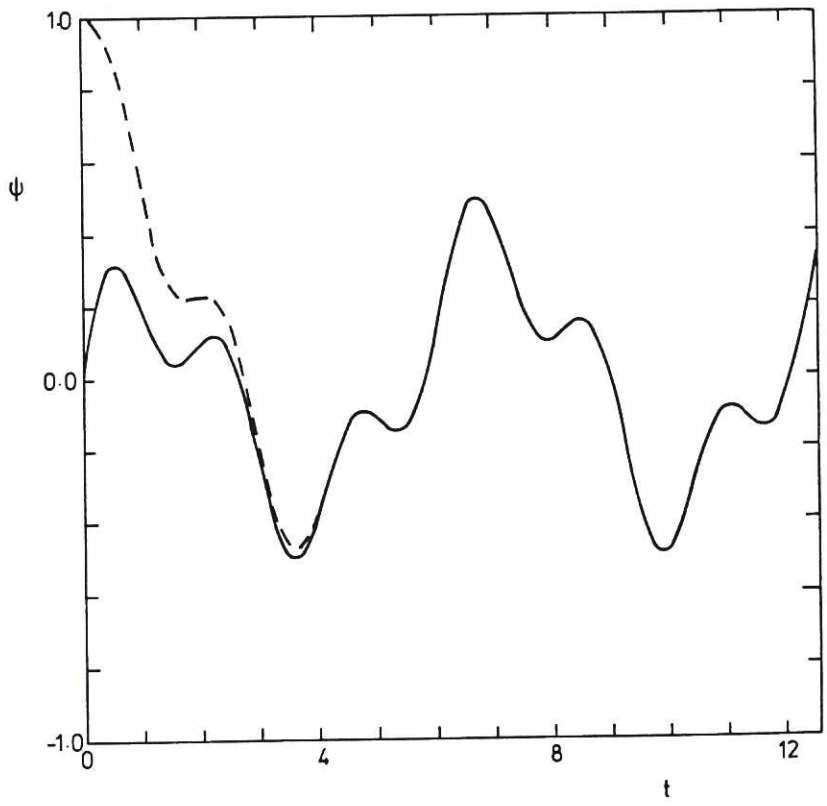

Fig. 3 The corresponding total flux ψ due to a simple resistive loop. The dashed curve shows the decay of the transient arising from the initial flux $\psi(0)=1$.

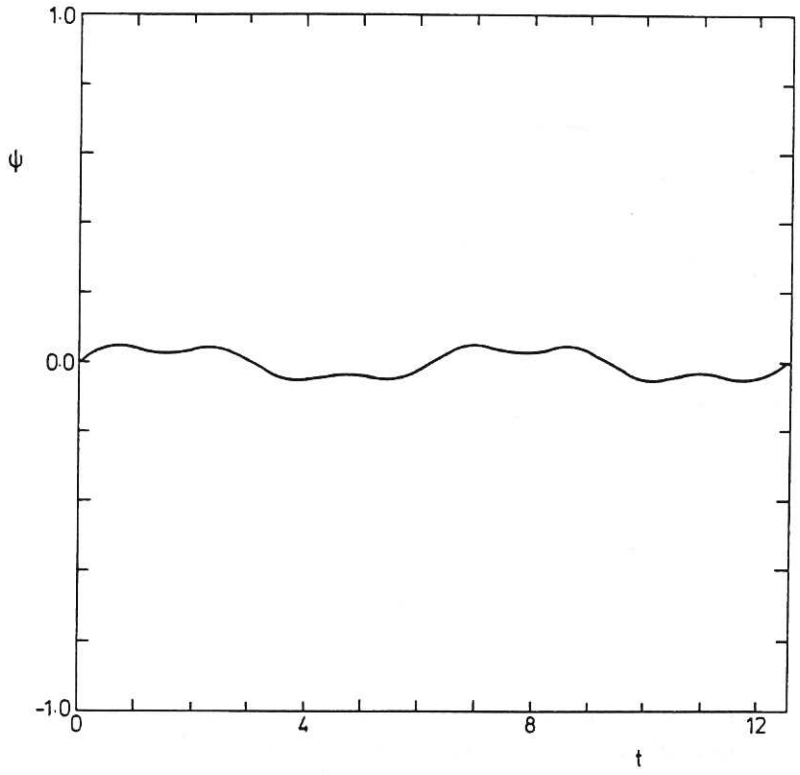

Fig. 4 Total flux with feedback amplification parameter $\alpha = 10$.

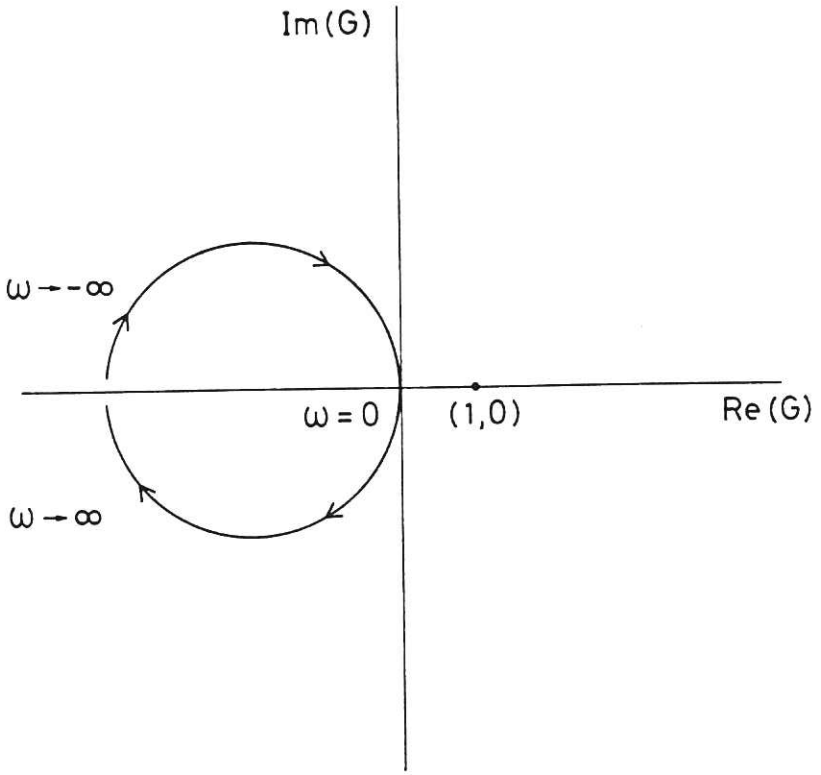

Fig. 5a Nyquist diagram for the open circuit response function $G(\omega)$ of the idealised amplifier of eq. (15) ($-\infty < \omega < \infty$).

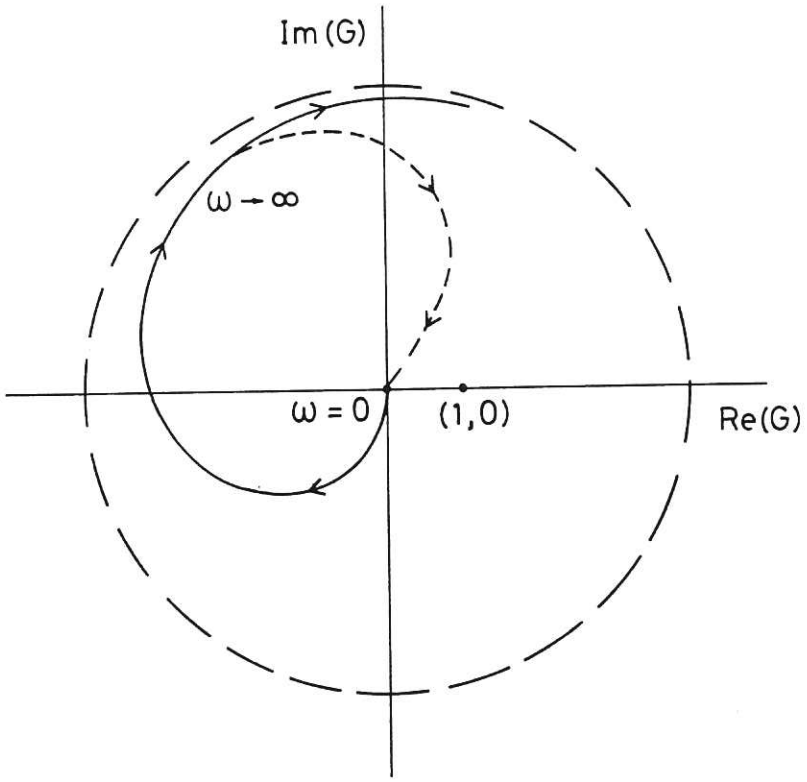

Fig. 5b The solid curve shows the Nyquist plot for an imperfect amplifier with time delay ($0 < \omega < \infty$). For $\omega \to \infty$ the curve approaches the outer circle and encloses the point (1,0) many times. Stability is restored by reducing the gain of the amplifier at large frequencies (dashed curve).

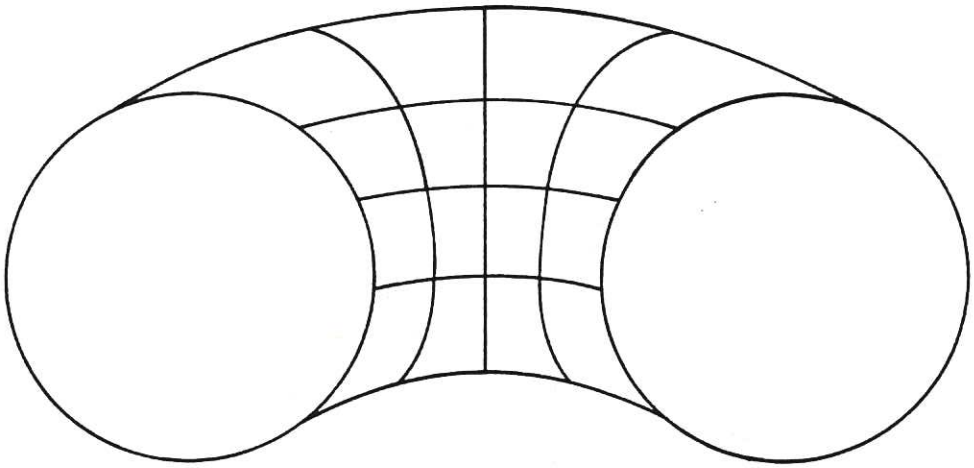

Fig. 6 A toroidal pinch surrounded by an Intelligent Shell.

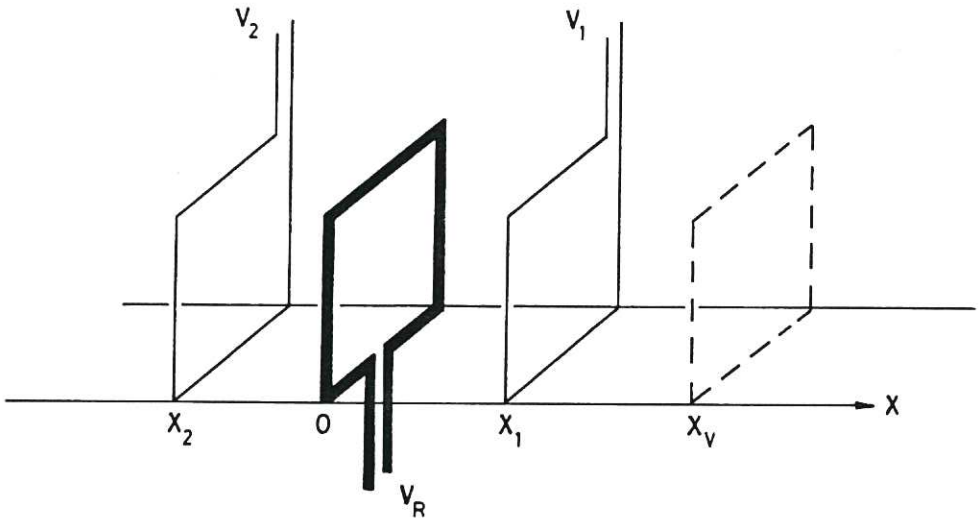

Fig. 7 This shows two sensing loops and a power loop displaced so as to create a virtual loop at $x = x_v$; (the spacing of the loops has been exaggerated for clarity).

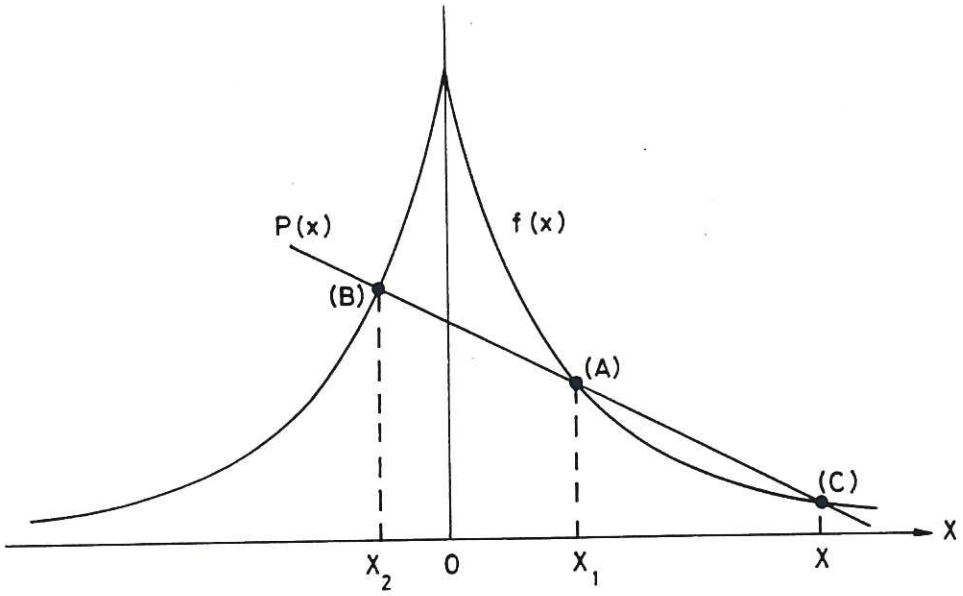

Fig. 8 Graphical solution of eq. (33).